QUANTITATIVE NDE OF THE YOUNG'S MODULUS OF FCC POROUS METALS

O. Yeheskel

Nuclear Research Centre Negev
P.O. Box 9001, Beer Sheva, 84190, Israel

Abstract

The present work manifests the results of the dynamic Young's modulus, *E*, after cold compaction and after sintering of partially dense copper and silver compacts. For both metals, the results show that *E* in the porous compacts depends not only on the attained density, but also on the samples' consolidation route. For porous metals, it is demonstrated that the normalized longitudinal sound wave velocity, V_L*, is more appropriate than porosity, for quantitative nondestructive evaluation (*NDE*) of the normalized Young's modulus, *E**. The proposed model uses, V_L*, to evaluate: $E^* \cong [\alpha V_L^{*3}+(1-\alpha)V_L^{*2}]C(\nu)$, where *a* is a constant defined from the compaction behavior, and $C(\nu)$, is a function of the Poisson's ratio, ν. This model was further verified for the normalized Young's modulus of porous nickel compacts.

Key words: Metals, Young's modulus, sound velocity, porosity, nondestructive evaluation

1. Introduction

The elastic moduli of porous materials have been studied both theoretically and experimentally during the last six decades [1-4]. Having porosity defined as the volume fraction of pores in a solid bulk, one may intuitively assume that the elastic moduli of porous materials decrease with porosity. This assumption was verified both theoretically and experimentally [1-9]. Various equations were put forward to describe the elastic moduli-porosity relations [2-9]. Such expressions devised for use as quantitative nondestructive evaluation (*QNDE*) of the elastic moduli of porous materials. Recent reports clearly indicate that the elastic moduli of porous materials are dependent not only on their density but also on the processing route that was followed [4,10-12]. The outcome of this finding is that for similar porosity values, there are various elastic moduli values [3,10-12]. These findings make the NDE based on porosity, inadequate.
Recently a *QNDE* approach for the elastic moduli of porous iron was introduced [4]. In this approach, a single sound wave velocity (SWV) is used for evaluating the elastic moduli of the porous metal.
The present study uses the same approach for the evaluation of the elastic moduli of few porous face centered cubic, FCC, metals (Ag, Cu, and Ni).

2. Methodology

The Young's moduli presented in the present work were calculated based on measuring the density , ρ, and time of flight or resonant frequency. The basis of dynamic methods is measuring either the resonant frequency or the time of flight of an acoustic wave traveling in the material. Using the samples dimensions, the sound velocities are derived [13].

2.1 SWV and elastic moduli relationships

For isotropic and homogeneous polycrystalline materials the relation between the shear SWV, V_T, and the shear modulus, *G*, is [14,15]:

$$V_T = (G/r)^{1/2} \quad (1)$$

For the longitudinal SWV, V_L,, the relation to the elastic properties is[15]:

$$V_L = (E/r)^{1/2}[(1-n)/(1+n)(1-2n)]^{1/2} \quad (2)$$

where *E* and ν are the Young's modulus and the Poisson's ratio, respectively. Poisson's ratio is defined as $\nu = E/2G - 1$ [14,15].
For manifestation purpose, we use the normalized properties *e.g.*: the Young's modulus, $E^*=E/E_B$; SWV, $V_L^*=V_L/V_{LB}$; and relative density, $\rho^*=\rho/\rho_{th}$. Where E_B, V_{LB} and ρ_{th} are the properties of the

pore-free solid bulk. Table 1, gives the room temperature, theoretical density, ρ_{th}, and elastic moduli for pore-free, Ag, Cu and Ni. For the former two materials, the properties were calculated from single crystal elastic moduli constants, using the Voigt-Ruess-Hill (VRH) approximation [16]. For Ni the results are from [17].

2.2 Young's moduli measurements

For the elastic moduli of Ag and Cu we used the pulse-echo method described elsewhere [10,11,18]. Other results for copper attained from Buch *et al.* [19] for long rods, using the density and the sonic velocity, V_S, often refer to as "bar velocity" [15], $E=\rho V_S^2$ [19]. For Ni the sonic velocity was used [20,21].

Table 1: The theoretical density, the elastic moduli, and the sound velocities of pore-free polycrystalline aggregates of: Ag [16], Cu, [16], and Ni [17].

	Ag	Cu	Ni
ρ_T [kgm^{-3}]	10530	8960	8910
G [GPa]	29.6	47.3	80
E [GPa]	81.1	127.1	214
ν	0.369	0.345	0.336
V_L [ms^{-1}]	3686	4726	6040
V_T [ms^{-1}]	1677	2298	3000
V_S [ms^{-1}]	-	-	4900

2.3 Samples preparations

2.3.1 Copper

Copper samples were either cold isostatically pressed (CIP'ed), or sintered according to the procedure given elsewhere [11]. Besides these samples, hot isostatic pressing (HIP) at 545°C and at 50 MPa was undertaken. For comparison we present the results of Buch *et al.* for Cu sintered for 2,4,8 and 16h, at 0.9 T_m, where T_m is the melting temperature in K [19].

2.3.2 Silver

Ag samples consolidated by cold pressed at various pressures. Prior to powder pressing, the powder was acid treated in a process designated as acid assisted consolidated (AAC) [10,22]. Few samples were cold pressed without AAC. Some samples either cold pressed or AAC, underwent sintering [10]. More results on AAC samples appear elsewhere [22].

2.3.3 Nickel

Ni powders were CIP'ed in the pressure range of 100-1330 MPa [20]. Sintering of the samples was conducted in the temperature range of 300-900°C. The details of sintering process appear elsewhere [20,21].

3. Results

3.1 Change of E^* and V_L^* with relative density

3.1.1 Copper

Fig. 1a and Fig. 1b show the variation of the normalized Young's modulus, E^*, and of the normalized longitudinal SWV, V_L^* with the relative density, respectively. In the current work, we use the longitudinal SWV, V_L. In order to use Buch *et al.*, V_S results, we transform them to V_L using [15]:

$$V_L = V_S[(1-n)/(1+n)(1-2n)]^{1/2} \quad (3)$$

In order to transform V_S to V_L values one should use the Poisson's ratio. Since Buch *et al.* did not provide ν values, we used approximate ν based on our results in the relative density range $0.75<\rho^*<1$, $\nu\sim0.10+0.24\rho^*$ (see later in Fig. 4a). Few features are apparent in Fig. 1a, the Young's modulus of our samples sintered at 0.5-0.8T_m for few minutes are similar to those of Buch *et al.* sintered at 0.9 T_m for few hours.

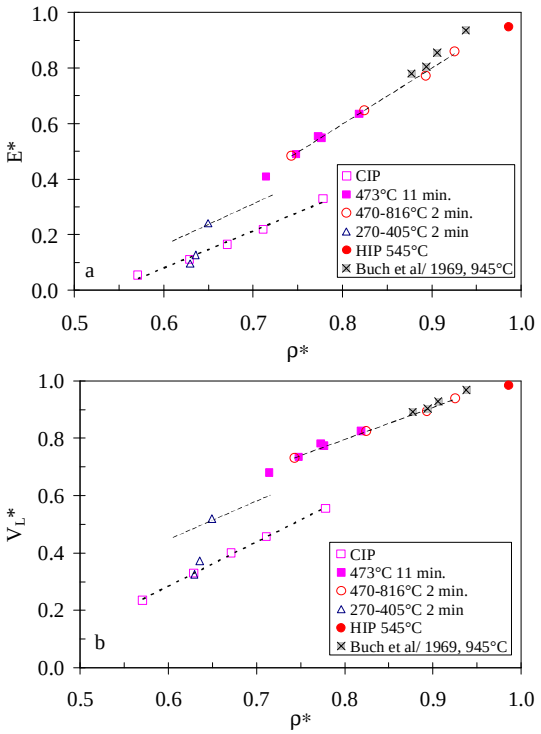

Fig. 1: The change of E^* (a) and of V_L^* (b) with the relative density of Cu samples.

This similarity probably stem from the similar nature of the interparticle boundaries in the two

cases. We recently claimed that the nature of the interparticle boundary change upon heating, resulting in improve of the elastic moduli [10,11]. Another finding is that the CIP'ed samples have much lower Young's modulus than the sintered samples. That this is due to the physical contact at the interparticle boundaries of the CIP'ed samples[11]. The sharp increase of E^* after short time sintering at 0.5 T_m is attributed to neck formation as verified by TEM work [11]. Similar behavior occurs for the change of V_L^* *vs.* ρ* (Fig. 1b). It seems that there is a linear correlation between V_L^* and. ρ*. The linear relation depends also on the sintering state [4]:

$$V_L^S* = V_L^C* + \Delta V_L^{CS}* \qquad (4)$$

where V_L^S* is the normalized SWV of the sintered sample, the term V_L^C* is the normalized SWV of the CIP'ed sample and the term, $\Delta V_L^{CS}*$, is the increase of the normalized SWV due to the sintering process. Similar description holds for the elastic moduli [4,11].

3.1.2 Silver

The variation of the E^*, and of V_L^* with relative density is given in Fig. 2a and Fig. 2b, respectively. It is evident that the change of E^*, and V_L^* with ρ*, is similar. The differences in samples preparation that yield the variation of the results extensively described elsewhere [10].
The fact that the results of Dariel *et al*. [22], lie along the same line of our results designated as powder A', stem from the similarity in preparation procedures.

3.1.3 Nickel

Fig. 3 shows the change of the normalized Young's modulus with the normalized density of Ni samples in the sintered state, CIP'ed state and in two intermediated states of heating [20,21]. Based on the similarity in the change E^*, and V_L^* *vs.* ρ*, in Fig. 1 Fig. 2, we omit in Fig. 3, the V_S^* *vs.* ρ* plot, to avoid redundancy.

3.2 Quantitative NDE

3.2.1 Basic approach

Nondestructive evaluation (NDE) is an important technique for assessing materials properties and structural integrity. For quantitative NDE of the elastic properties of porous substances, we rely on the theory of elasticity. Any elastic modulus, M, can be determined from two independent elastic moduli [14]. One may also represent any elastic modulus, using single SWV and one independently measured elastic modulus [14]. Hence, M is [4]:

$$M = rV_L^2 f_{LM}(n) \qquad (5)$$

where $f_{LM}(n)$ is a function of the Poisson's ratio that correlates M with V_L. Details of these functions for the various elastic moduli for both V_L and V_T, are given elsewhere [4]. If one succeeds expressing both, ρ(V_L) and ν(V_L), a description of any elastic modulus utilizing, V_L, becomes possible.
We start with an expression of the density in terms of SWV:

$$r = (aV_L + b) \qquad (6)$$

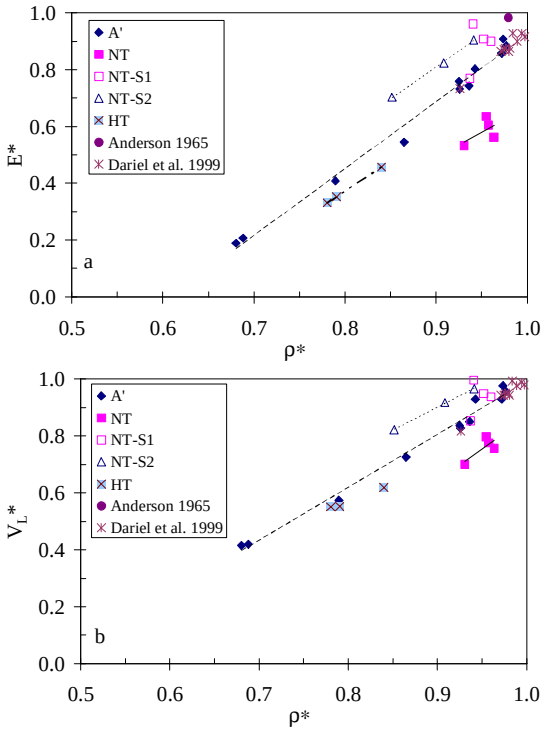

Fig. 2: (a) The change of E^* with ρ* of porous Ag samples. (b) The change of V_L^* with ρ* for the same samples.

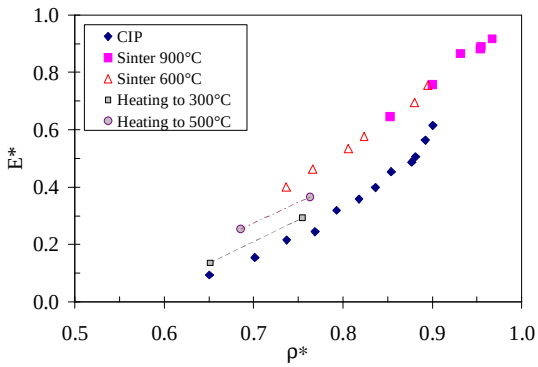

Fig. 3: The change of E^* with the relative density of Ni samples [20,21].

where a is a slope that represents the change of V_L with respect to ρ, and b is the intercept for $V_L \rightarrow 0$. By using the normalized version, we get:

$$r^* \cong (aV_L^* + b) \qquad (7)$$

where α = a/(a+b) and β = b/(a+b). It is easy to show that β = (1-α).

From Eq. (2) ones gets the Young's modulus:

$$E = rV_L^2 f_{LE}(n) \qquad (8)$$

where $f_{LE}(\nu)=(1+\nu)(1-2\nu)/(1+\nu)$. Introducing Eq. (7) and $\rho=\rho_{th}\rho^*$, into Eq. (8) yield:

$$E \cong r_{th}(aV_L^* + b)V_L^2 f_{LE}(n) \qquad (9)$$

For the case of normalized Young's modulus, we get $E^*=E/E_B$:

$$E^* \cong [aV_L^{*3} + (1-a)V_L^{*2}]C(n) \qquad (10)$$

where $C(\nu) = (f_{LE}/ f_{LEB})$ where f_{LEB} is the function for the case of pore-free material [4].

3.2.2 Poisson's ratio

Now we will show that $\nu(V_L)$, is possible. The common assumption for porous materials is that the Poisson's ratio is insensitive to density variations [5,19]. Fig. 4a and Fig. 4b show the change of the Poisson's ratio in copper with the change of the relative density and the normalized SWV, respectively. Fig. 5a and Fig. 5b show the changes in the Poisson's ratio for silver as in Fig. 4.
For both materials the Poisson's ratio changes by about 100% in the density range $0.65<\rho^*\leq 1.0$. For the purpose of our *QNDE* approach, we can fairly evaluate the Poisson's ratio, in the SWV range $0.35<V_L^*\leq 1.0$, by either power or a linear relationships of ν and V_L^*. Fig. 4b and Fig. 5b show such relations. The power relationship is [4]:

$$n_{EV} \cong n_B V_L^{*m} \qquad (11)$$

where ν_{EV} is the evaluated Poisson's ratio of the porous material, ν_B is the Poisson's ratio for the pore-free substance, and m is a coefficient calculated using least square analysis. The calculated m values are about 0.6 and 0.8 for copper and silver, respectively. For both metals, the evaluated Poisson's ratio may be expressed as:

$$n_{EV} \cong c + dV_L^* \qquad (12)$$

where c and d are coefficients calculated using least square analysis. The values of c and d for both Cu and Ag appear in Fig. 4b and Fig. 5b, respectively.

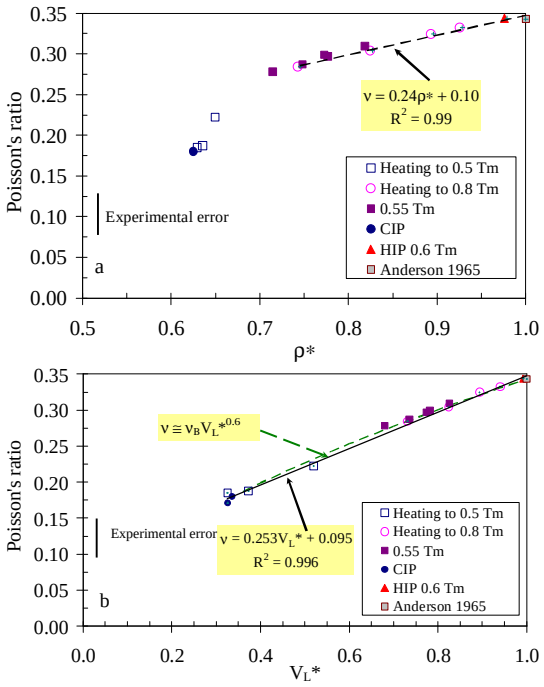

Fig. 4: The variation of the Poisson's ratio in porous Cu compacts, a) with the relative density, b) with the normalized longitudinal SWV.

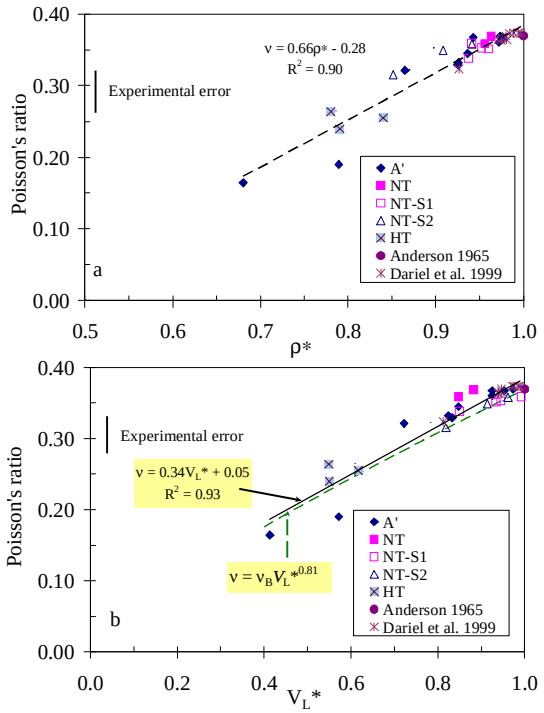

Fig. 5: The variation of the Poisson's ratio in porous Ag compacts, a) with the relative density, b) with the normalized longitudinal SWV.

3.2.3 The term C(ν)

The term needed for describing E^* in terms V_L^*, is $C(\nu)= (f_{LE}/ f_{LEB})$. f_{LEB} is easily calculated by introducing ν_B (Table 1) into $f_{LE}(\nu)= (1+\nu)(1-2\nu)/(1+\nu)$. While for estimation of f_{LE} , we use an evaluated value of the Poisson's ratio from either Eq. (11) or Eq. (12).

3.3 Evaluation of Young's modulus

3.3.1 Copper

Fig. 6 show the Young's moduli of the Cu compacts shown in Fig. 1a, when plotted against V_L^*. For plotting Fig. 6, the values the slope of the sintered samples above 405°C, were used yielding α=0.723. Three evaluation lines representing three cases appear in Fig. 6 and in Fig. 7.

Case I - Stand for Eq. (10) for which the $C(\nu)$ values are based on evaluation of ν_{EV} from Eq. (11).

Case II - Stand for Eq. (10) for which we drive $C(\nu)$based on evaluation of ν_{EV} from Eq. (12).

Case III - Stand for Eq. (10) for which omit $C(\nu)$, in order to check its significance.

The lines representing Case-I, and Case- II, give good evaluations of E^*, (±0.05). The line representing Case–III, describes the general change of E^* *vs.* V_L^*, but underestimates the measured E^* values in the range $0.4<V_L^*<0.8$, by more than 0.05.

3.3.2 Silver

Fig. 7 show the Young's moduli of the Ag compacts shown in Fig. 2a, when plotted against the normalized SWV. The entire E^* data points seem to increase monotonously with V_L^*. For the *QNDE* procedure in Fig. 7, the slope of the data points designated by A', were used yielding, α=0.521.

The line for Case-I, describes all the data points with uncertainty of ± 0.05. For Case II, the line predicts the data points very well, but deviates downward at $V_L^*\rightarrow 1.0$, to $E^*=0.92$ which is inadequate. For Case-III, Fig. 7 shows large deviations of the predicted from the measured values, *e.g.* in the range $0.4<V_L^*<0.8$, deviations of E^* are about 0.07 to 0.15.

3.3.3 Nickel

Fig. 8 show the Young's moduli of the Ni compacts shown in Fig. 3, when plotted against V_S^*. In Fig. 8 we used the values of the data points of CIP'ed samples, *i.e.* α=0 58. However in the case of Ni we use the sonic velocity for which f_{SE} = 1. Therefore, Eq. (10) becomes:

$$E^* \cong [a V_S^{*3} + (1-a) V_S^{*2}] \qquad (13)$$

The line representing Eq. (13) in Fig. 8, gives very good evaluations of all the E^* values.

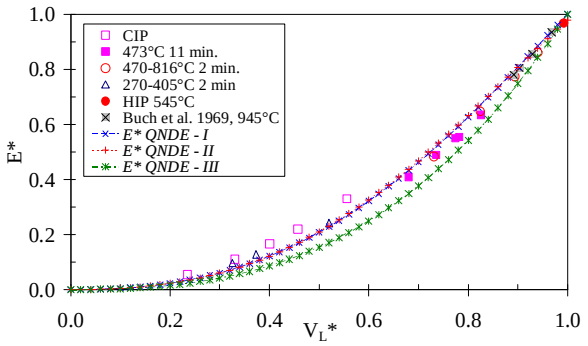

Fig. 6: Quantitative NDE of E^* based on the V_L^* of porous Cu compacts.

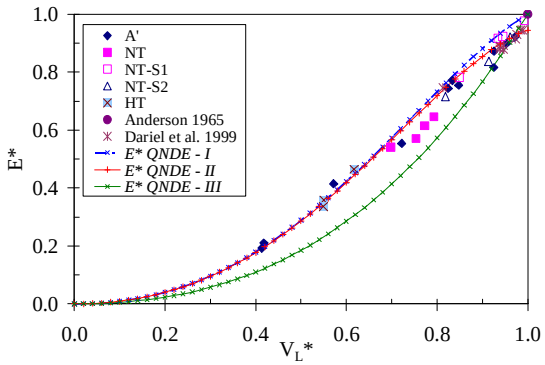

Fig. 7: Quantitative NDE of E^* based on the V_L^* of porous Ag compacts.

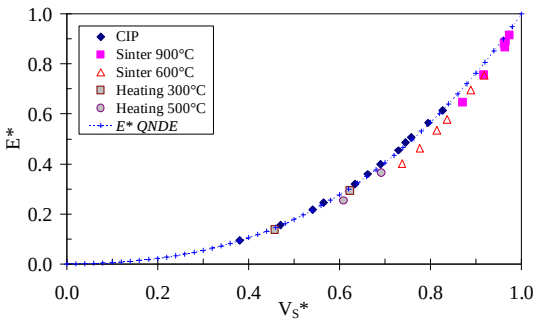

Fig. 8: The change of the normalized Young's moduli of porous Ni compact with the normalized sonic velocity.

4. Conclusions

In the present study, we show that the Young's moduli of some FCC porous metals (Cu, Ag, Ni), depend besides on the density, also on their consolidation route. We here by devise the equation that relates the Young's moduli to a single sound velocity, either the longitudinal SWV, V_L, or the sonic velocity, V_S. This becomes possible by introducing an equation that correlates the density and the sound velocity. Another important finding is the proposed evaluation methods of the Poisson's ratio of porous compacts based on the normalized SWV. There two possible ways to correlates the Poisson's ratio to V_L*. One is a linear relation given in Eq. (11). The second is power relation given in Eq. (12).

The general equation, for *QNDE* of the Young's modulus of porous metallic compacts is based on replacing density by a function of SWV, and introducing the Poisson's ratio based on SWV. This gives an equation where E* increases monotonously with V_L*. The total deviations between the measured and predicted values are in the range of ±0.05 of E*. Such deviations are more than fair for quantitative NDE method.

References

[1] Mackenzie, J.K. "The elastic constants of a solid containing spherical holes", *Proc. Phys. Soc.* (London) Series B 63, 2-11,1950.

[2] McAdam, G.D., "Some relations of powder characteristics to the elastic modulus and shrinkage of sintered ferrous compacts", *Journal of the Iron and Steel Institute*, 168(4): 346-358, 1951.

[3] Knudsen, F. P., " Effect of porosity on Young's modulus of alumina", *J. American Ceramic Society*, 45(2): 94-95, 1962.

[4] Yeheskel O., Nondestructive Evaluation of the Dynamic Elastic Moduli of Porous Iron Compacts, *J. Testing and Evaluation*, 32 (1): 17-23, 2004.

[5] Wang, J. C. "Young's Modulus of Porous Materials, Part I: Theoretical derivation of modulus- porosity correlation", *J. Materials Science*, 19: 801-808, 1984.

[6] Rice, R. W. "Effects of inhomogeneous porosity on elastic properties of ceramics", *J. American Ceramic Society*, 58(9): 458-459, 1975.

[7] Dean E.A. and Lopez, J.A., "Empirical dependence of elastic moduli on porosity for ceramic materials", *J. American Ceramic Society*, 66(5): 366-370,1983.

[8] Jeong H.and Hsu, D.K. "Quantitative estimation of material properties of porous ceramics by means of composite micromechanics and ultrasonic velocity", *NDT&E International*, 29 (2): 95-101, 1996.

[9] Ondrecek, G., "The quantitative microstructure-field property correlation of multiphase and porous materials", Reviews on Powder Metallurgy and Physical ceramics, 3 (3&4): 205-322, 1987, KFK-4566, *Kernforschungzentrum Karlsruhe* March 1989.

[10] Yeheskel, O., Ratzker, M., Shokhat, M.and Dariel, M.P.," Elastic constants of porous silver compacts after acid assisted consolidation at room temperature", *J. Material Science*, 36: 1219-1225, 2001.

[11] Yeheskel, O., Pinkas M., and Dariel, M.P., "Evolution of the elastic moduli at the early stage of copper sintering", *Materials Letters* 57: 4418-4423, 2003.

[12] Tevet, O., and Yeheskel, O., "Quantitative Non-Destructive Evaluation (QNDE) of the Elastic Moduli of Porous Al_2O_3", *Key Engineering Materials*, 224-226: 835-840, 2002.

[13] Standard practice for Measuring Ultrasonic Velocity in Materials, ASTM designation E 494-95 March 1995.

[14] Ledbetter, H.M., and Reed, R.P., "Elastic Properties of Metals and Alloys, I. Iron., Nickel and Iron-Nickel Alloys", *J. Physical and Chemical Reference Data*, 12(3): 531-616, 1973.

[15] Timoshenko, S. P. , Goodier, J.N., Theory of Elasticity, McGraw-Hill book Co., New York, 1972.

[16] Anderson, O. L., "Determination of some uses of isotropic elastic constants of polycryst- alline aggregates using single-crystal data", in Mason, W.P. editor, Physical Acoustics, Vol.-III part B, Academic Press, New York, 43-95, 1965.

[17] Mason W. P, Physical Acoustics and the Properties of Solids, D. Van Nostrand Co. Inc. Princeton New Jersey, 1958, p. 17.

[18] Yeheskel, O., Tevet, O., "Elastic moduli of transparent yttria",*J. American Ceramic Society*, 82(1): 136-144, 1999.

[19] Buch, A and Goldschmidt, S., "Influence of porosity on elastic moduli of sintered materials", *Materials Science and. Engineering*, 5: 111-118 1969/70.

[20] Cytermann, R.,"A new way to investigate the dependence of elastic moduli on the microstructure of porous materials", Powder Metallurgy International ,19 [4], 27-30 ,1987.

[21] Cytermann, R., Thèse de docteur ingénieur "Applications de la stereologie a l'étude des propriétés physiques et mécaniques de corps poreux", L'Université de Paris sud, Dec.1978.

[22] Dariel, M.P., Ratzker, M., and Eichmiller, F.C., "Acid-assisted consolidation of powder compacts:

cold-welding or cold sintering**"** *J. Material. Science*, .34: 2601-2607, 2001.